EurJOC
European Journal of Organic Chemistry

Research Article
doi.org/10.1002/ejoc.202400408

Chemistry Europe
European Chemical Societies Publishing

www.eurjoc.org

# Fusion of Cyclohepta[*def*]fluorene Units: Toward Synthesis of High-Spin Non-Benzenoid Nanographenes

Fupeng Wu,[a, b] Yubin Fu,[a, b] Wenhui Niu,[a, b] Fupin Liu,[c, e] Renxiang Liu,[b] Zhenlin Qiu,[b] Alexey A. Popov,[c] Junzhi Liu,[d] Ji Ma,*[a, b] and Xinliang Feng*[a, b]

Non-benzenoid diradicaloids possessing high-spin ground states are attractive synthetic targets given their high potential for spintronics and quantum computing. Nevertheless, the synthesis of such compounds remains highly challenging due to their inherent instability. In this work, we present the synthetic attempt towards creating a non-benzenoid diradicaloid (**1**) with a triplet ground state by fusing two cyclohepta[*def*]fluorene units onto a benzene ring. Our synthetic approach involves both oxidation and reduction pathways. In the oxidation path, we obtained the partially dehydrogenated products **1+H** and **1+2H** containing an indeno[1,2-*b*]fluorene core from the tetrahydro precursor (**2**). However, further dehydrogenation to afford the target molecule (**1**) did not proceed. On the other hand, with the reduction pathway, a novel tetraketone precursor (**9**) with two pairs of pentagons and heptagons was successfully synthesized. The subsequent nucleophilic attack however was proved to be difficult probably due to the unselective nucleophilic addition on the zigzag nanographene ketones. Furthermore, UV-vis absorption, cyclic voltammetry, and theoretical calculations were conducted to explore the optical, electrochemical properties, and aromaticity of all the obtained molecules (**1+H**, **1+2H** and **9**). Although the desired target **1** is not achieved, our work provides insight into designing novel high-spin non-benzenoid NGs based on nonalternant cyclohepta[*def*]fluorene system.

## Introduction

Open-shell nanographenes (NGs), or extended polycyclic hydrocarbons (PHs), exhibiting a high-spin ground state, are garnering significant interest due to their promising applications in opto-electronics, organic spintronics, and quantum computing.[1–7] This high-spin ground state is predominantly observed in non-Kekulé systems, limited to the triangulenes mainly prepared by on-surface synthesis under ultrahigh vacuum conditions.[8–12] In contrast, non-benzenoid Kekulé systems may also manifest an open-shell high-spin ground state, accessible through topological engineering of the molecular backbone of PHs.[13–18] As a representative example of a non-benzenoid system, indenofluorene, composed of a conjugated array of fused 6-5-6-5-6 rings, serves as an interesting case study.[19–26] The five indenofluorenes isomers (**a**–**e**) result in a wide range of computed diradical character values from $y_0 = 0.021$ for the closed-shell singlet indeno[2,1-*c*]fluorene (**a**) to $y_0 = 0.645$ for the open-shell singlet indeno[2,1-*b*]fluorene (**d**) then to the large $y_0 = 0.987$ for the open-shell triplet indeno[1,2-*a*]fluorene (**e**) (Figure 1a), in which their electronic ground state were also proved by experimental results.[18a] However, non-benzenoid high-spin diradicaloids have remained largely inaccessible thus far due to the challenging synthesis caused by their high reactivities, as well as the absence of suitable building units.

Recently, the introduction of non-alternant units (i.e., azulene or heptalene) in the skeleton of NGs appears to be a promising strategy for achieving the low highest occupied molecular orbital and lowest unoccupied molecular orbital (HOMO–LUMO) splitting, potentially leading to the access to high-spin ground state in non-benzenoid NGs.[27–35] For example, cyclohepta[*def*]fluorene (Figure 1b), one of seven non-alternant pyrene isomers, was early predicted to possess an open-shell nature with a triplet ground state.[36,37] Until 2022, Our group[28] and Yasuda's group[38] independently reported the synthesis of cyclohepta[*def*]fluorene derivatives, including the triaryl derivative (**g**) and the benzo-extended analogue (**h**), respectively. However, the experiment results showed that both of them have the singlet ground state with a low-lying triplet state. Consequently, the well-established Lieb's theorem and Ovchin-

[a] Dr. F. Wu, Dr. Y. Fu, Dr. W. Niu, Dr. J. Ma, Prof. Dr. X. Feng
Max Planck Institute of Microstructure Physics
Weinberg 2, 06120 Halle, Germany
E-mail: ji.ma@mpi-halle.mpg.de
xinliang.feng@tu-dresden.de

[b] Dr. F. Wu, Dr. Y. Fu, Dr. W. Niu, R. Liu, Dr. Z. Qiu, Dr. J. Ma, Prof. Dr. X. Feng
Center for Advancing Electronics Dresden (cfaed) & Faculty of Chemistry and Food Chemistry
Technische Universität Dresden
Mommsenstrasse 4, 01062 Dresden (Germany)

[c] Dr. F. Liu, Dr. A. A. Popov
Leibniz Institute for Solid State and Materials Research
Helmholtzstraße 20, 01069 Dresden (Germany)

[d] Dr. J. Liu
Department of Chemistry and State Key Laboratory of Synthetic Chemistry
The University of HongKong, Hong Kong (China)

[e] Dr. F. Liu
Department School of Chemistry and Materials Science,
Nanjing Normal University, 210023 Nanjing (China)

Supporting information for this article is available on the WWW under https://doi.org/10.1002/ejoc.202400408

Research Article
doi.org/10.1002/ejoc.202400408



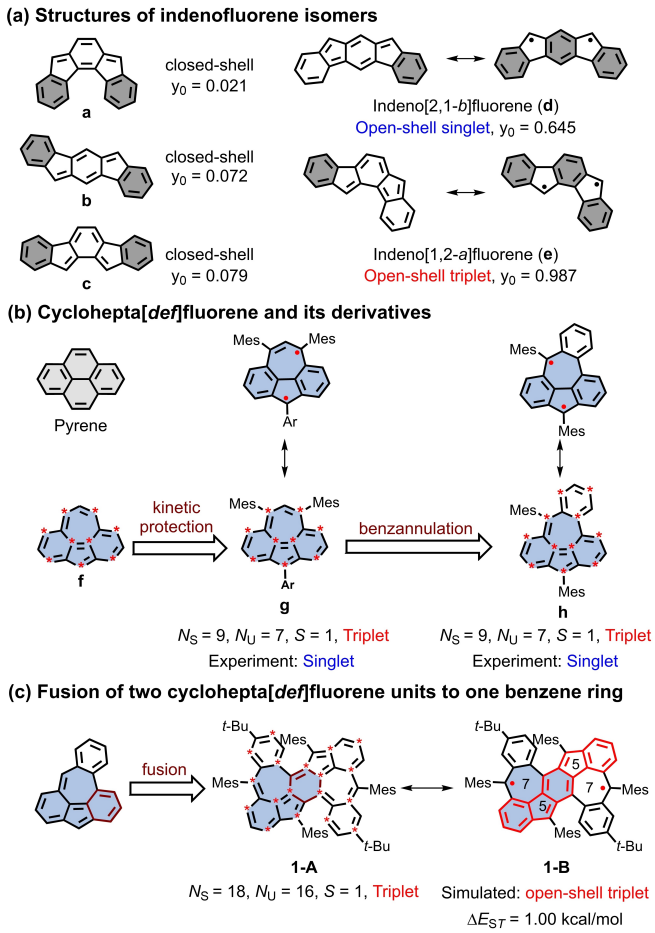


**Figure 1.** (a) Resonance structures of indenofluorene isomers in closed- and open-shell forms, with Clar's sextets highlighted in black. The biradical character indices ($y_0$) are listed according to reported references.[18a] (b) The structure of cyclohepta[def]fluorene derivatives. (c) Fusion of two cyclohepta[*def*]fluorene units onto one benzene ring. Spin nature of ground state (*S*) is anticipated by the extension of Ovchinnikov rule ($S = (Ns\text{-}Nu)/2$, *Ns* and *Nu* are present number of starred and unstarred atoms, respectively).

nikov rule do not effectively apply in non-benzenoid π-systems, and accessing the triplet ground state in non-alternant systems remains a challenging task, which motivates us to explore the design and synthesis of other novel non-benzenoid NGs based on the cyclohepta[*def*]fluorene system.

Herein, we report our endeavors towards the synthesis of a novel non-benzenoid diradicaloid, dibenzo[3,4:6,7]azuleno[8,1-*ab*]benzo[6,7]cyclohepta[1,2,3,4-*def*]fluorene (**1**) (Figure 1c). Our approach entails the lateral fusion of two cyclohepta[def]fluorene units onto a single benzene ring, where the gain of four Clar's sextets in the open-shell form, overcomes the electron pairing in **1**. As predicted by the extension of the Ovchinnikov rule[39] and DFT calculations, **1** possesses an open-shell triplet ground state with a singlet-triplet energy gap ($\Delta E_{ST}$) of 1.00 kcal/mol (Figure S9). Based on different strategies utilized in the final step to generate the radicals, our synthetic approach includes both oxidation and reduction pathways. In the oxidation pathway, we successfully synthesized a tetrahydro precursor (**2**), that is, a derivative of 4,9,13,18-tetrahydrodibenzo[3,4:6,7]azuleno[8,1-*ab*]benzo[6,7]cyclohepta[1,2,3,4-*def*]fluorene. Unfortunately, the final dehydrogenation to target **1** failed despite the enormous efforts, yielding partially dehydrogenated byproducts **1**+**H** and **1**+**2H** based on the indeno[1,2-*b*]fluorene backbone. It is proposed that **1**+**H** is an open-shell monoradical, exhibiting good stability under ambient conditions ($t_{1/2}$ = 122 h). For the reduction pathway, we successfully achieved a novel tetraketone precursor **9** with two pairs of pentagons and heptagons. However, the subsequent nucleophilic addition reaction did not proceed as expected possibly due to the nucleophilic attack at the α-carbon in a 1,4-addition manner.[40] Moreover, the optical and electrochemical properties, electronic structures, and aromaticity of the obtained products (**1**+**H**, **1**+**2H** and **9**) have been fully investigated by UV-vis absorption and cyclic voltammetry as well as DFT calculations. This work enriches the structural diversity of indeno[1,2-*b*]fluorene-based non-alternant NGs and provides insightful guidance for the design and synthesis of non-benzenoid NGs with high-spin ground states.

## Results and Discussion

The first synthesis attempt for the targeted diradicaloid (**1**) involves oxidative dehydrogenation as the key step. As shown in Scheme 1, a Suzuki coupling reaction between commercially available 1,4-dibromo-2,5-diiodobenzene (**3**) and (4-(*tert* butyl)phenyl)boronic acid (**4**) gave 2′,5′-dibromo-4,4′′-di-tert-butyl-1,1′:4′,1′′-terphenyl (**5**) in 78% yield. Then, a Suzuki coupling between compound **5** and the reported 2-(4,4,5,5-tetramethyl-1,3,2-dioxaborolan-2-yl)isophthalaldehyde (**6**)[28] yielded the key intermediate 2′,5′-bis(4-(*tert*-butyl)phenyl)-[1,1′:4′,1′′-terphenyl]-2,2′′,6,6′′-tetracarbaldehyde (**7**) in 42% yield. Afterwards, compound **7** was treated with an excess of 2-mesitylmagnesium bromide to give the diol, which was then subjected to Friedel-Crafts alkylation promoted by $BF_3{\cdot}OEt_2$ to afford the key tetra-hydro **2** with a yield of 51% in two steps. The formation of the pentagon-heptagon in this step leads to four stereocenters and thus forms stereoisomers of **2**. As detailed in Table S1, various oxidative agents, solvents, reaction temperatures, and reaction time were evaluated in the oxidative dehydrogenation of **2**, in which the reaction progress was monitored by matrix-assisted laser desorption/ionization time-of-flight (MALDI-TOF) mass spectrometry. Different reagents, including tetrachloro-1,4-benzoquinone (TCBQ), 2,3-dichloro-5,6-dicyanobenzoquinone (DDQ), and potassium *tert*-butoxide, were used to facilitate the oxidative dehydrogenation, but only a partial dehydrogenation product **1**+**H** or **1**+**2H** were detected. Additionally, a step-by-step synthesis method was also explored, commencing with the dehydrogenation reaction of compound **2**, followed by the oxidation of the partially dehydrogenated product **1**+**2H** using various oxidative agents. However, similar to previous attempts, only some partially dehydrogenated or oxidized products were observed. Furthermore, attempts were made to remove the two remaining hydrogen atoms from compound **1**+**2H** to generate a dication, followed by the oxidation reaction to

Research Article
doi.org/10.1002/ejoc.202400408



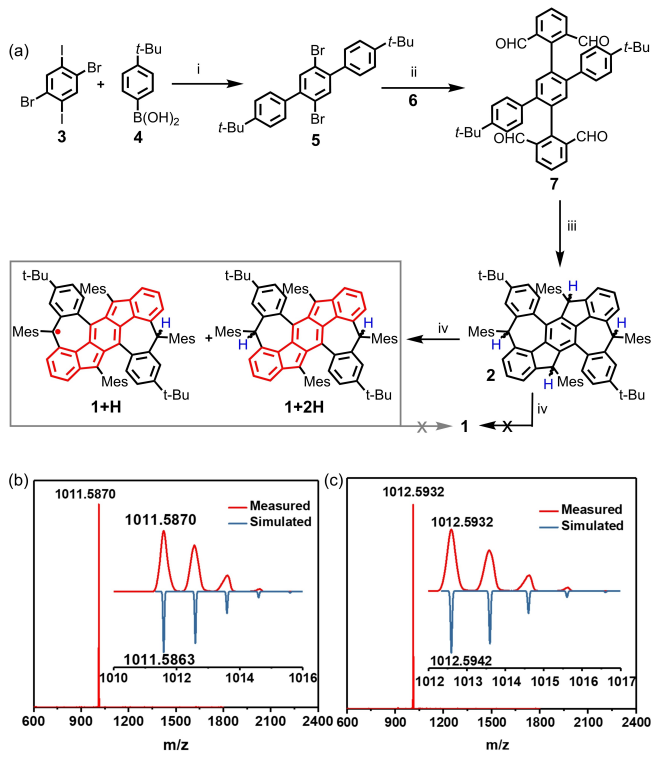


**Scheme 1.** (a) Towards synthesis of high spin diradicaloid (**1**) via oxidative dehydrogenation approach. Reagents and conditions: (i) $Pd(PPh_3)_4$, $K_2CO_3$, 1,4-dioxane, 90 °C, 24 h, 78%. (ii) 2-(4,4,5,5-tetramethyl-1,3,2-dioxaborolan-2-yl)isophthalaldehyde (**6**), $Pd_2(dba)_3$, SPhos, $K_3PO_4$, Toluene/THF, 100 °C, 48 h, 42%. (iii) 2-mesitylmagnesium bromide, THF, RT, overnight; then $BF_3{\cdot}OEt_2$, $CH_2Cl_2$, RT, 40 min; 51% in two steps. (iv) Different entry. Detailed reagents and conditions of the oxidative dehydrogenation reaction are shown in Table S1. HR MALDI-TOF MS of b) **1**+**H** and c) **1**+**2H**. Inset: experimental (red solid line) and simulated (blue solid line) isotopic distribution patterns of the mass peak.

yield the target product (**1**). However, the reaction did not proceed when treated with triphenylcarbenium tetrafluoroborate (Table S1, Entry 23). Nevertheless, the partially dehydrogenated byproducts **1**+**H** and **1**+**2H** could be achieved under the optimized reaction condition using four equivalents of DDQ, chlorobenzene as the solvent, and stirring at room temperature overnight (Table S1, Entry 15). After the reaction, compounds **1**+**H** and **1**+**2H** could be separated and purified by silica column chromatography. HR MALDI-TOF mass spectra of **1**+**H** and **1**+**2H** show only one dominant peak, displaying isotopic distribution patterns that closely match their simulated spectra. (Scheme 1b and 1c).

The structure of **1**+**2H** was further confirmed by single crystal analysis, in which its single crystal was obtained by slow evaporation of its dichloromethane/methanol solution. In principle, compound **1**+**2H** has two stereocenters, one at the pentagon and another at the heptagon, leading to four possible isomers. However, only the *cis*-isomer of **1**+**2H** was observed in its single-crystal structure (Figure S2–S3). It is noteworthy to mention that both **1**+**H** and **1**+**2H** feature a quinoid structures in their indenofluorene backbones, which could contribute to stabilizing the structures. Additionally, compounds **1**, **1**+**H** and **1**+**2H** contain two pentagon-heptagon units and have the non-planar backbone, with the mesityl-substitutions perpendicular to the molecular skeleton (Figure 2 and Figure S5).

The UV–vis absorption spectra of **1**+**2H** and **1**+**H** in anhydrous DCM solutions are illustrated in Figure 3a. The absorption spectrum of **1**+**2H** exhibited a broad absorption

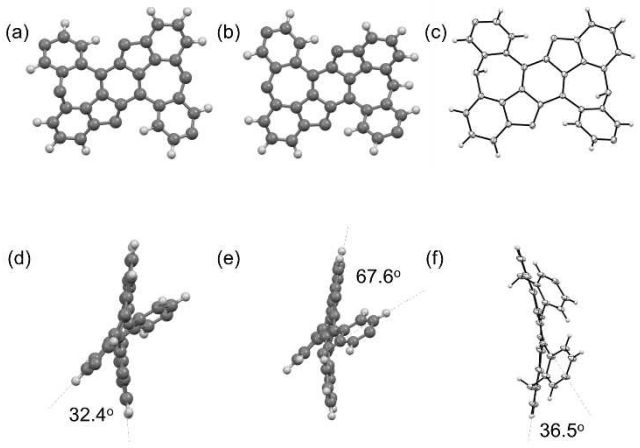


**Figure 2.** Optimized (UB3LYP/6-31G(d)) structures of **1** and **1**+**H** as well as X-ray crystallographic structure of **1**+**2H**. Top view (a) **1**, (b) **1**+**H**, (c) **1**+**2H**. Side view (d) **1**, (e) **1**+**H**, (f) **1**+**2H**. All mesityl and *t*-Bu substituents are omitted for clarity. Values show a dihedral angle of the non-planar geometry structure.

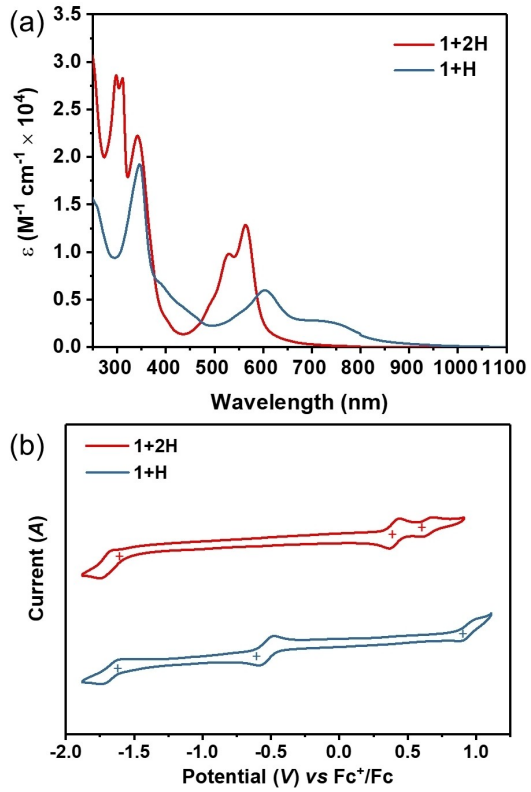


**Figure 3.** (a) UV–vis absorption spectra of **1**+**H** and **1**+**2H** in DCM ($10^{-4}$ M). (b) Cyclic voltammograms of **1**+**H** and **1**+**2H** in DCM containing 0.1 M n-$Bu_4NPF_6$ at a scan rate of 0.1 V $s^{-1}$. Ferrocene was used as an external standard.

Research Article
doi.org/10.1002/ejoc.202400408



range from 450 to 650 nm, attributed to the absorption of the quinoid structure in the indenofluorene backbone. Specifically, compound **1+2H** shows purple color in the solution state (Figure S7) and displays a maximum absorption peak ($\lambda_{max}$) at 564 nm, with an absorption onset at 601 nm, corresponding to an optical energy gap ($E_g^{opt}$) of 2.06 eV, which aligns with values reported for 6,12-diarylindeno[1,2-*b*]fluorenes derivatives ($E_g^{opt}$: 2.05–2.20 eV).[41] In contrast, compound **1+H** exhibited a deep green color in the solution state. Compared to **1+2H**, the UV-vis-NIR absorption spectra of **1+H** in DCM solution show a low-energy light absorption band with an onset absorption wavelength of 1011 nm (Figure 3a). According to the time-dependent density-functional theory (TD-DFT) calculations (Figure S12 and Table S4), this weak and low-energy absorption is a transition involving the singly occupied molecular orbital (SOMO), which can be attributed to its open-shell character. From the onset wavelength of the absorption, the optical energy gap of **1+H** is estimated to be 1.23 eV. In addition, time-dependent UV-vis-NIR spectra show that **1+H** has persistent stability under ambient conditions (Figure S8), with a half-life time $t_{1/2}=$ 122 h. Furthermore, the electrochemical behavior of **1+2H** and **1+H** were investigated by cyclic voltammetry (CV) in anhydrous DCM. As illustrated in Figure 3b, **1+2H** featured two reversible oxidation waves with half-wave potential $E^{ox}_{1/2}$ values at 0.44 and 0.69 V, and one reversible reduction wave with an $E^{red}_{1/2}$ at −1.75 V. However, **1+H** displayed one quasi-reversible oxidation wave with $E^{ox}_{1/2}$ values at 0.99 V, and two reversible reduction waves with an $E^{red}_{1/2}$ at −0.59 V and −1.74 eV. The HOMO/LUMO levels were estimated to be −5.14 eV/−3.23 eV and −5.64 eV/−4.36 eV for **1+2H** and **1+H**, respectively, according to the onset potentials of the first oxidation/reduction waves. The electrochemical energy gaps ($E_g^{CV}$) were thus calculated to be 1.91 and 1.28 eV for **1+2H** and **1+H**, respectively, which are in good accordance with their optical energy gaps. Similar to the optical energy gap, the $E_g^{CV}$ of **1+2H** also aligns well with the reported range for 6,12-diarylindeno[1,2-b]fluorene derivatives (1.88–2.22 eV).[41] The smaller band gap of compound **1+H** may be attributed to its open-shell character. In addition, the theoretical hyperfine coupling constants (HFCCs) of **1+H** were estimated by DFT calculations (Figure S9), and the electron paramagnetic resonance (EPR) spectrum of **1+H** in the toluene solution was conducted. However, a detailed analysis of **1+H** signal was not possible because of its superimposition with the strong EPR signal from $DDQ^{\bullet-}$ impurities (Figure S10).

Given the unsuccessful attempts in the oxidation pathway, an alternative synthetic route for the targeted diradicaloid (**1**) was developed, which involves the reduction of the key tetra-ketone precursor **9** in the final step. As depicted in Scheme 2, the tetra-aldehyde **7** was first oxidized by potassium permanganate ($KMnO_4$), yielding the tetracarboxylic acid **8** in a quantitative yield. Initially, cyclization to form compound **9** was unsuccessful when using concentrated sulfuric acid or methanesulfonic acid. However, by combining methanesulfonic acid with 10% polyphosphoric acid (PPA),[42] the cyclization of **8** was accomplished to afford tetra-ketone

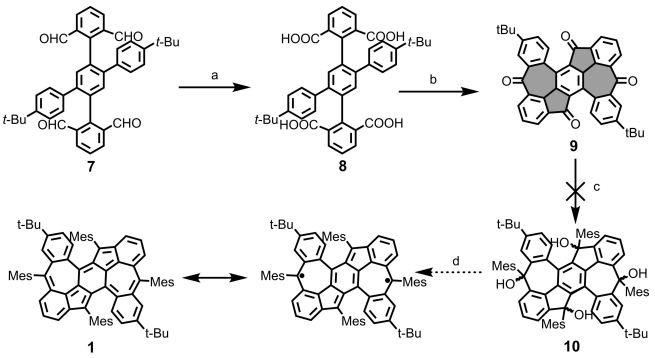


**Scheme 2.** Towards synthesis of **1** via the reduction approach. Reagents and conditions: (a) $KMnO_4$, acetone/$H_2O$, 60 °C, 24 h, quant. (b) 10% wt PPA/MsOH, 120 °C, 2 h, 56%. (c) 2-mesitylmagnesium bromide, THF, RT, overnight. (d) $SnCl_2$, DCM.

**9** in 56% yield. The chemical structure of compound **9** was first confirmed by mass spectrometry and NMR spectroscopy. Notably, the single crystal of **9** was obtained by slow evaporation of its dichloromethane/methanol solution. As shown in Figure 4a, tetra-ketone **9** also features two pentagon-heptagon pair units, with two seven-membered rings incorporated into indeno[1,2-b]fluorene-6,12-dione, leading to a non-planar geometry characterized by a dihedral angle of 34.9° (Figure S6). With tetraketone **9** in hand, nucleophilic attack on **9** with 2-mesitylmagnesium bromide was attempted. Unfortunately, the reaction did not produce the desired tetra-alcohol **10**; instead, various complex side-products were formed, which may arise from a nucleophilic attack on the $\alpha$-carbon in a 1,4-addition reaction.[40] Consequently, the final reduction reaction of **9** to the high spin diradicaloid (**1**) was not realized.

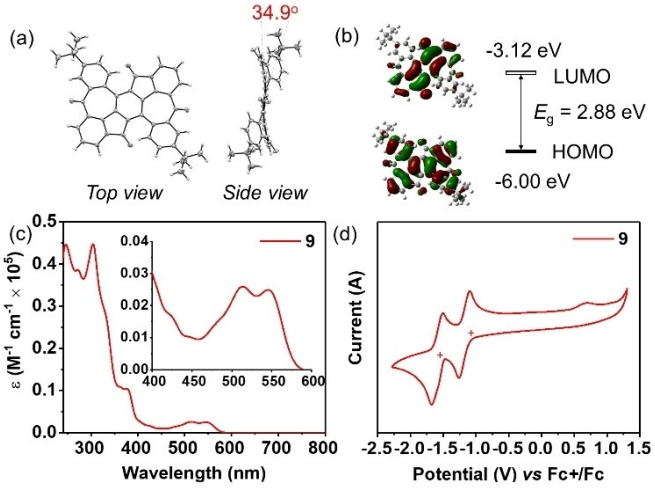


**Figure 4.** (a) Top view and side view of the X-ray crystallographic structure of **9** (ORTEP drawing with at the 50% probability level). (b) Molecular orbitals and the energy diagrams of **9** calculated at the B3LYP/6-31G(d) level. (c) UV-vis absorption spectrum of **9** in DCM ($10^{-5}$ M). The inset shows the zoom-in spectrum of 400 to 600 nm. (d) Cyclic voltammograms of **9** in DCM containing 0.1 M $n$-$Bu_4NPF_6$ at a scan rate of 0.1 $V s^{-1}$. Ferrocene was used as an external standard.

According to the DFT calculation, compound **9** shows deep energy levels of HOMO and LUMO (calculated values: −6.00 eV/−3.12 eV, Figure 4b) due to the presence of four ketone groups that have strong electron-withdrawing ability. The UV–vis absorption spectrum of **9** in anhydrous DCM solution is presented in Figure 4c. The spectrum of **9** showed a $\lambda_{max}$ at 514 and 546 nm and an absorption onset at 578 nm, corresponding to an optical energy gap of 2.15 eV. The electrochemical behavior of **9** was also investigated by CV in anhydrous DCM. As shown in Figure 4d, compound **9** displayed two reversible reduction waves with a half-wave potential $E^{red}_{1/2}$ of −1.26 V and −1.68 (vs Fc+/Fc) and did not show any oxidation process within the anodic potential range. The HOMO/LUMO energy level of **9** was estimated to be −5.85 eV/−3.70 eV based on the onset potentials of the reduction waves and the optical energy gap. The deep HOMO level is in accordance with the calculated results.

To gain deeper insight into electronic structures of **1**, **1+H** and **1+2H**, DFT calculations at the R/UB3LYP/6-31G(d) level were performed. Both compounds **1** and **1+H** are open-shell molecules and **1** has a triplet ground state (Figure S11). In contrast, compound **1+2H** is calculated to be closed-shell molecule, which is consistent with the experimental results. To further analyze the aromaticity of **1**, **1+H**, **1+2H** and **9**, nucleus-independent chemical shift (NICS)[43] and anisotropy of the induced current density (ACID)[44] calculations at the B3LYP/6-311+G(d,2p) level of theory were performed (Figure S13–16). In these four molecules, all the $NICS(1)_{zz}$ values of non-hexagonal rings (pentagons and heptagons) are positive, suggesting their antiaromatic character (Figure 5, a–c and Figure S13–15). This antiaromatic character of non-benzenoid rings is distinct from that of azulene, in which both pentagonal and heptagonal rings show aromatic character. Interestingly, the middle benzene ring of **1**, **1+H** and **1+2H** also exhibits positive $NICS(1)_{zz}$ values, which differ from that of indeno[1,2-*b*]fluorene. Moreover, these results are further supported by the anticlockwise ring current flow in the non-benzenoid rings and the diatropic ring current circuits in the peripheral benzene rings, as shown in ACID maps (Figure 5d–f and Figure S13–15).

## Conclusions

In summary, we detail our endeavors toward the synthesis of a novel azulene-embedded open-shell diradicaloid (**1**) with an intrinsic triplet ground state, which can be viewed as the lateral fusion of two cyclohepta[*def*]fluorene units onto a single benzene ring. We proposed two synthetic strategies, involving oxidation and reduction approaches, aimed at generating the diradicaloid **1**. In the oxidation route, only the partially dehydrogenated products **1+H** and **1+2H** with an indeno[1,2-*b*]fluorene core were obtained from tetrahydro precursor (**2**). However, further dehydrogenation to afford the target molecule (**1**) did not proceed. With the reduction pathway, a novel tetraketone precursor (**9**) with two pairs of pentagons and heptagons was obtained. These derivatives represent novel indenofluorene-based non-benzenoid PHs characterized by a quinoid structure in the molecular backbone. Furthermore, optical and electronic chemical properties of **1+H**, **1+2H** and **9** were thoroughly investigated. Additionally, the calculated NICS and ACID results suggest the antiaromatic character of the embedded non-benzenoid rings for **1+H**, **1+2H** and **9**. This work enriches the structural diversity of indeno[1,2-*b*]fluorene-based derivatives and provides valuable guidance for the design and synthesis of open-shell non-benzenoid NGs with high-spin ground states.

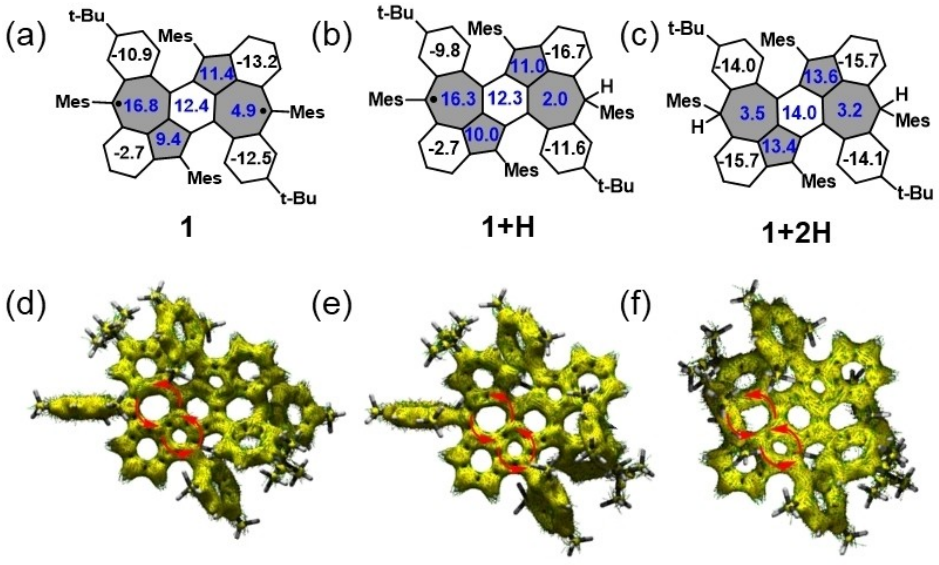


**Figure 5.** NICS(1)zz values (a–c) and ACID plots (d–f) of **1**, **1+H** and **1+2H**, respectively. The non-hexagonal rings were highlighted in black color. The anticlockwise ring current flow on one of two pentagon-heptagon units is shown with red arrow.

## Supporting Information

The authors have cited additional references within the Supporting Information.[46–55]

## *Acknowledgements*

This research was financially supported by the EU Graphene Flagship (Graphene Core 3, 881603), ERC Consolidator Grant (T2DCP, 819698), H2020-MSCA-ITN (ULTIMATE, No. 813036), the Center for Advancing Electronics Dresden (cfaed), H2020-EU.1.2.2.-FET Proactive Grant (LIGHT-CAP, 101017821), and the DFG-SNSF Joint Switzerland-German Research Project (EnhanTopo, No. 429265950). The authors gratefully acknowledge the GWK support for funding this project by providing computing time through the Center for Information Services and HPC (ZIH) at TU Dresden. Diffraction data have been collected on BL14.2 at the BESSY II electron storage ring operated by the Helmholtz-Zentrum Berlin, we thank the team of Dr. Manfred Weiss for supporting the experiment at BESSY II. We also thank Dr. Evgenia Dmitrieva (IFW Dresden) for the EPR measurement and helpful discussions. Open Access funding enabled and organized by Projekt DEAL.

## *Conflict of Interests*

The authors declare no conflict of interest.

**Keywords:** open-shell · polycyclic hydrocarbons · high spin · non-benzenoid · indenofluorene

[1] I. Ratera, J. Veciana, *Chem. Soc. Rev.* **2012**, *41*, 303–349.
[2] C. Shu, H. Zhang, A. Olankitwanit, S. Rajca, A. Rajca, *J. Am. Chem. Soc.* **2019**, *141*, 17287–17294.
[3] Z. Y. Wang, Y. Z. Dai, L. Ding, B. W. Dong, S. D. Jiang, J. Y. Wang, J. Pei, *Angew. Chem. Int. Ed.* **2021**, *60*, 4594–4598.
[4] F. Lombardi, A. Lodi, J. Ma, J. Liu, M. Slota, A. Narita, W. K. Myers, K. Müllen, X. Feng, L. Bogani, *Science* **2019**, *366*, 1107–1110.
[5] S. Mishra, G. Catarina, F. Wu, R. Ortiz, D. Jacob, K. Eimre, J. Ma, C. A. Pignedoli, X. Feng, P. Ruffieux, *Nature* **2021**, *598*, 287–292.
[6] F. Lombardi, J. Ma, D. I. Alexandropoulos, H. Komber, J. Liu, W. K. Myers, X. Feng, L. Bogani, *Chem* **2021**, *7*, 1363–1378.
[7] S. Mishra, D. Beyer, K. Eimre, S. Kezilebieke, R. Berger, O. Gröning, C. A. Pignedoli, K. Müllen, P. Liljeroth, P. Ruffieux, *Nat. Nanotechnol.* **2020**, *15*, 22–28.
[8] S. Arikawa, A. Shimizu, D. Shiomi, K. Sato, R. Shintani, *J. Am. Chem. Soc.* **2021**, *143*, 19599–19605.
[9] S. Mishra, D. Beyer, K. Eimre, J. Liu, R. Berger, O. Gröning, C. A. Pignedoli, K. Müllen, R. Fasel, X. Feng, *J. Am. Chem. Soc.* **2019**, *141*, 10621–10625.
[10] J. Su, M. Telychko, P. Hu, G. Macam, P. Mutombo, H. Zhang, Y. Bao, F. Cheng, Z.-Q. Huang, Z. Qiu, *Sci. Adv.* **2019**, *5*, eaav7717.
[11] S. Mishra, K. Xu, K. Eimre, H. Komber, J. Ma, C. A. Pignedoli, R. Fasel, X. Feng, P. Ruffieux, *Nanoscale* **2021**, *13*, 1624–1628.
[12] J. Su, M. Telychko, S. Song, J. Lu, *Angew. Chem. Int. Ed.* **2020**, *59*, 7658–7668.
[13] T. Kubo, *Chem. Rec.* **2015**, *15*, 218–232.
[14] S. Das, J. Wu, *Phys. Sci. Rev.* **2017**, *2*.
[15] Y. Huang, E. Egap, *Polym. J.* **2018**, *50*, 603–614.
[16] W. Zeng, J. Wu, *Chem* **2021**, *7*, 358–386.
[17] T. Y. Gopalakrishna, W. Zeng, X. Lu, J. Wu, *Chem. Commun.* **2018**, *54*, 2186–2199.
[18] a) M. Di Giovannantonio, K. Eimre, A. V. Yakutovich, Q. Chen, S. Mishra, J. I. Urgel, C. A. Pignedoli, P. Ruffieux, K. Müllen, A. Narita, *J. Am. Chem. Soc.* **2019**, *141*, 12346–12354; b) C. K. Frederickson, B. D. Rose, M. M. Haley, *Acc. Chem. Res.* **2017**, *50*, 977–987.
[19] D. T. Chase, B. D. Rose, S. P. McClintock, L. N. Zakharov, M. M. Haley, *Angew. Chem. Int. Ed.* **2011**, *50*, 1127.
[20] A. Shimizu, Y. Tobe, *Angew. Chem.* **2011**, *30*, 7038–7042.
[21] A. G. Fix, P. E. Deal, C. L. Vonnegut, B. D. Rose, L. N. Zakharov, M. M. Haley, *Org. Lett.* **2013**, *15*, 1362–1365.
[22] A. Shimizu, R. Kishi, M. Nakano, D. Shiomi, K. Sato, T. Takui, I. Hisaki, M. Miyata, Y. Tobe, *Angew. Chem. Int. Ed.* **2013**, *52*, 6076–6079.
[23] J. J. Dressler, Z. Zhou, J. L. Marshall, R. Kishi, S. Takamuku, Z. Wei, S. N. Spisak, M. Nakano, M. A. Petrukhina, M. M. Haley, *Angew. Chem.* **2017**, *129*, 15565–15569.
[24] J. J. Dressler, M. Teraoka, G. L. Espejo, R. Kishi, S. Takamuku, C. J. Gomez-Garcia, L. N. Zakharov, M. Nakano, J. Casado, M. M. Haley, *Nat. Chem.*. **2018**, *10*, 1134–1140.
[25] G. E. Rudebusch, J. L. Zafra, K. Jorner, K. Fukuda, J. L. Marshall, I. Arrechea-Marcos, G. L. Espejo, R. Ponce Ortiz, C. J. Gomez-Garcia, L. N. Zakharov, *Nat. Chem.*. **2016**, *8*, 753–759.
[26] C. K. Frederickson, B. D. Rose, M. M. Haley, *Acc. Chem. Res.* **2017**, *50*, 977–987.
[27] S. Mishra, D. Beyer, R. Berger, J. Liu, O. Gröning, J. I. Urgel, K. Mullen, P. Ruffieux, X. Feng, R. Fasel, *J. Am. Chem. Soc.* **2020**, *142*, 1147–1152.
[28] F. Wu, J. Ma, F. Lombardi, Y. Fu, F. Liu, Z. Huang, R. Liu, H. Komber, D. I. Alexandropoulos, E. Dmitrieva, *Angew. Chem.* **2022**, *134*, e202202170.
[29] F. Wu, A. Barragán, A. Gallardo, L. Yang, K. Biswas, D. Écija, J. I. Mendieta-Moreno, J. I. Urgel, J. Ma, X. Feng, *Chem. Eur. J.* **2023**, *29*, e202301739.
[30] H. Miyoshi, S. Nobusue, A. Shimizu, Y. Tobe, *Chem. Soc. Rev.* **2015**, *44*, 6560–6577.
[31] Y. Tobe, *Chem. Rec.* **2015**, *15*, 86–96.
[32] A. Konishi, M. Yasuda, *Chem. Lett.* **2021**, *50*, 195–212.
[33] S. H. Pun, Q. Miao, *Acc. Chem. Res.* **2018**, *51*, 1630–1642.
[34] Y. Tobe, *Chem. Rec.* **2015**, *15*, 86–96.
[35] Y. Fei, J. Liu, *Adv. Sci.* **2022**, *9*, 2201000.
[36] M. Nendel, B. Goldfuss, K. N. Houk, K. Hafner, U. Grieser, *Theor. Chem. Acc.* **1999**, *102*, 397–400.
[37] K. Horii, P. Baumgartner, E. Weltin, G. Wagnière, E. Heilbronner, *Helv. Chim. Acta* **1965**, *48*, 751–764.
[38] K. Horii, R. Kishi, M. Nakano, D. Shiomi, K. Sato, T. Takui, A. Konishi, M. Yasuda, *J. Am. Chem. Soc.* **2022**, *144*, 3370–3375.
[39] A. A. Ovchinnikov, *Theor. Chim. Acta* **1978**, *47*, 297–304.
[40] P. Ribar, L. Valenta, T. Šolomek, M. Juriček, *Angew. Chem. Int. Ed.* **2021**, *60*, 13521–13528.
[41] D. T. Chase, A. G. Fix, S. J. Kang, B. D. Rose, C. D. Weber, Y. Zhong, L. N. Zakharov, M. C. Lonergan, C. Nuckolls, M. M. Haley, *J. Am. Chem. Soc.* **2012**, *134*, 10349–10352.
[42] C. Frederickson, L. Zakharov, M. M. Haley, *J. Am. Chem. Soc.* **2016**, *138*, 16827–16838.
[43] P. v. R. Schleyer, C. Maerker, A. Dransfeld, H. Jiao, N. J. van Eikema Hommes, *J. Am. Chem. Soc.* **1996**, *118*, 6317–6318.
[44] R. Herges, D. Geuenich, *J. Phys. Chem. A* **2001**, *105*, 3214–3220.
[45] CCDC numbers 2305551 (for **1**+**2H**), 2305550 (for **9**), contain the supplementary crystallographic data for this paper. These data are provided free of charge by the joint Cambridge Crystallographic Data Centre and Fachinformationszentrum Karlsruhe Access Structures service.
[46] Y.-K. Zhang, J. J. Plattner, E. E. Easom, D. Waterson, M. Ge, Z. Li, L. Li, Y. Jian, *Tetrahedron Lett.* **2011**, *52*, 3909–3911.
[47] J. Liu, A. Narita, S. Osella, W. Zhang, D. Schollmeyer, D. Beljonne, X. Feng, K. Müllen, *J. Am. Chem. Soc.* **2016**, *138*, 2602–2608.
[48] U. Mueller, R. Förster, M. Hellmig, F. U. Huschmann, A. Kastner, P. Malecki, S. Pühringer, M. Röwer, K. Sparta, M. Steffien, M. Ühlein, P. Wilk, M. S. Weiss, *Eur. Phys. J. Plus* **2015**, *130*, 141.
[49] W. Kabsch, *Acta Crystallogr. Sect. D* **2010**, *66*, 125–132.
[50] K. M. Sparta, M. Krug, U. Heinemann, U. Mueller, M. S. Weiss, *J. Appl. Crystallogr.* **2016**, *49*, 1085–1092.
[51] G. Sheldrick, *Acta Crystallogr. Sect. C* **2015**, *71*, 3–8.
[52] Gaussian 16, Revision C.01, M. J. Frisch, G. W. Trucks, H. B. Schlegel, G. E. Scuseria, M. A. Robb, J. R. Cheeseman, G. Scalmani, V. Barone, G. A. Petersson, H. Nakatsuji, X. Li, M. Caricato, A. V. Marenich, J. Bloino, B. G. Janesko, R. Gomperts, B. Mennucci, H. P. Hratchian, J. V. Ortiz, A. F. Izmaylov, J. L. Sonnenberg, D. Williams-Young, F. Ding, F. Lipparini, F. Egidi, J. Goings, B. Peng, A. Petrone, T. Henderson, D. Ranasinghe, V. G.

Research Article
doi.org/10.1002/ejoc.202400408



Zakrzewski, J. Gao, N. Rega, G. Zheng, W. Liang, M. Hada, M. Ehara, K. Toyota, R. Fukuda, J. Hasegawa, M. Ishida, T. Nakajima, Y. Honda, O. Kitao, H. Nakai, T. Vreven, K. Throssell, J. A. Montgomery, Jr., J. E. Peralta, F. Ogliaro, M. J. Bearpark, J. J. Heyd, E. N. Brothers, K. N. Kudin, V. N. Staroverov, T. A. Keith, R. Kobayashi, J. Normand, K. Raghavachari, A. P. Rendell, J. C. Burant, S. S. Iyengar, J. Tomasi, M. Cossi, J. M. Millam, M. Klene, C. Adamo, R. Cammi, J. W. Ochterski, R. L. Martin, K. Morokuma, O. Farkas, J. B. Foresman, and D. J. Fox, Gaussian, Inc., Wallingford CT, 2016.

[53] a) K. Yamaguchi, F. Jensen, A. Dorigo, K. N. Houk, *Chem. Phys. Lett.* **1988**, *49*, 537–542; b) K. Yamaguchi, Y. Takahara, T. Fueno, K. N. Houk, *Theor. Chim. Acta* **1988**, *73*, 337–364.

[54] R. Herges, D. Geuenich, *J. Phys. Chem. A* **2001**, *105*, 3214–3220.

[55] P. V. R. Schleyer, C. Maerker, A. Dransfeld, H. Jiao, N. J. van Eikema Hommes, *J. Am. Chem. Soc.* **1996**, *118*, 6317–6318.

Manuscript received: April 28, 2024
Accepted manuscript online: April 30, 2024
Version of record online: ■■, ■■

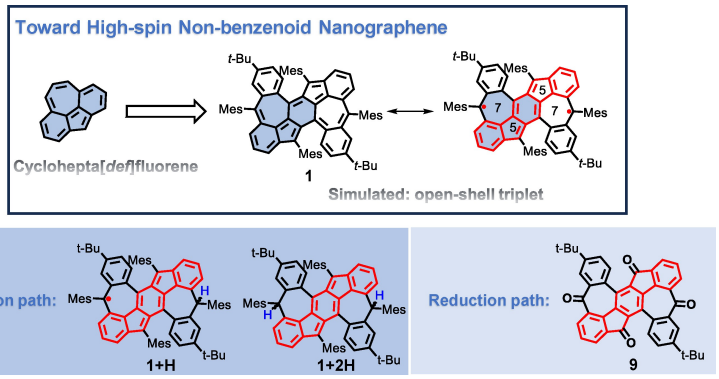


Non-benzenoid diradicaloid (**1**) with a triplet ground state was designed by fusing two cyclohepta[def]fluorene units onto one benzene ring. Our synthetic attempts towards **1** involve both oxidation and reduction pathways. In the oxidation path, partially dehydrogenated products **1**+**H** and **1**+**2H** containing an indeno[1,2-*b*]fluorene core were obtained. In the reduction path, a new tetraketone precursor (**9**) with two pairs of pentagons and heptagons was afforded.

*Dr. F. Wu, Dr. Y. Fu, Dr. W. Niu, Dr. F. Liu, R. Liu, Dr. Z. Qiu, Dr. A. A. Popov, Dr. J. Liu, Dr. J. Ma*, Prof. Dr. X. Feng**

1 – 8

**Fusion of Cyclohepta[*def*]fluorene Units: Toward Synthesis of High-Spin Non-Benzenoid Nanographenes**